

Biostratigraphical investigation of calcareous nannofossils: The middle Paleogene to early Neogene strata from the eastern parts of Iran (Median Tethys sea-way)

Mina Ghavidel Darestani¹, and Ahmad Reza Khazaei³

Received 17 June 2020; accepted 18 March 2021; published 29 August 2021.

In a complete succession obtained from southeast of Birjand, in the Eastern part of Iran, the open marine sediments have been deposited without any disconformity from Paleogene to early Neogene systems. We conducted the biostratigraphic investigations within this sedimentary succession according to calcareous nannofossils from the Roobiat Village section. Based on the calcareous nannofossil species index, we have detected the NP16 to NN3 zones and subzones which are comparable with the Martini biozonation pattern. Thus, we could suggest a middle Eocene (Bartonian) to early Miocene (Burdigalian) age for this section. Since the studied section contains a complete sedimentary sequence from Paleogene to Neogene systems, as a comparisonal section for the correlation between bio-horizons from western parts of the Tethys basin and its eastern parts, it is recommended. **KEYWORDS:** Biostratigraphy.

Citation: Darestani, Mina Ghavidel, and Ahmad Reza Khazaei (2021), Biostratigraphical investigation of calcareous nannofossils: The middle Paleogene to early Neogene strata from the eastern parts of Iran (Median Tethys sea-way), *Russ. J. Earth. Sci.*, 21, ES4006, doi:10.2205/2021ES000762.

1. Introduction

The Eocene and Oligocene are the geological time periods with significant changes in oceanic circulations and the global climate. A thick sequence of open marine sediments was deposited during this time in the Bagheran Mountains, a part of the Sistan suture zone, in Eastern part of Iran [Tirrul *et al.*, 1983]. The Sistan suture zone is one of the eastern structural-sedimentary zones of Iran that is located between Iran and Afghanistan. This zone is surrounded by two main faults, Nehban-

dan (to the west) and Harirud (to the east). It extends for 800 km from north to south and 200 km from east to west and contains thick volcanic and sedimentary rocks [Aghanabati, 2006]. This complicated zone displays the intensity of continental tectonics ensued from the displacement of Lut and Hillmand continental sheets, judging from their structural pattern. In the Sistan suture zone, the nature of the faults is mostly of overlapping drifts. It should be pointed out that although the north-northeast movements of the Arabian Plate along with the African plate affect the Iranian Plate in most parts, the Iranian Eastern Flysch Basin is mostly influenced by the movements of the Indian plate towards north-northwest and the consequences thereof. In other words, the formation of the Indian Ocean shapes most structures in this region [Berberian and King, 1981]. Previous reports [e.g. Aghanabati, 2006; Hadavi *et al.*, 2016; Jalili *et al.*, 2020], claim that the oldest rocks found in this area are from the Cretaceous. There-

¹Department of Geology, Faculty of Sciences, Ferdowsi University of Mashhad, Mashhad, Iran

²Department of Paleontology and Geochemistry research, Exploration directorate of NIOC, Tehran, Iran

³Department of Geology, Faculty of Sciences, University of Birjand, Birjand, Iran

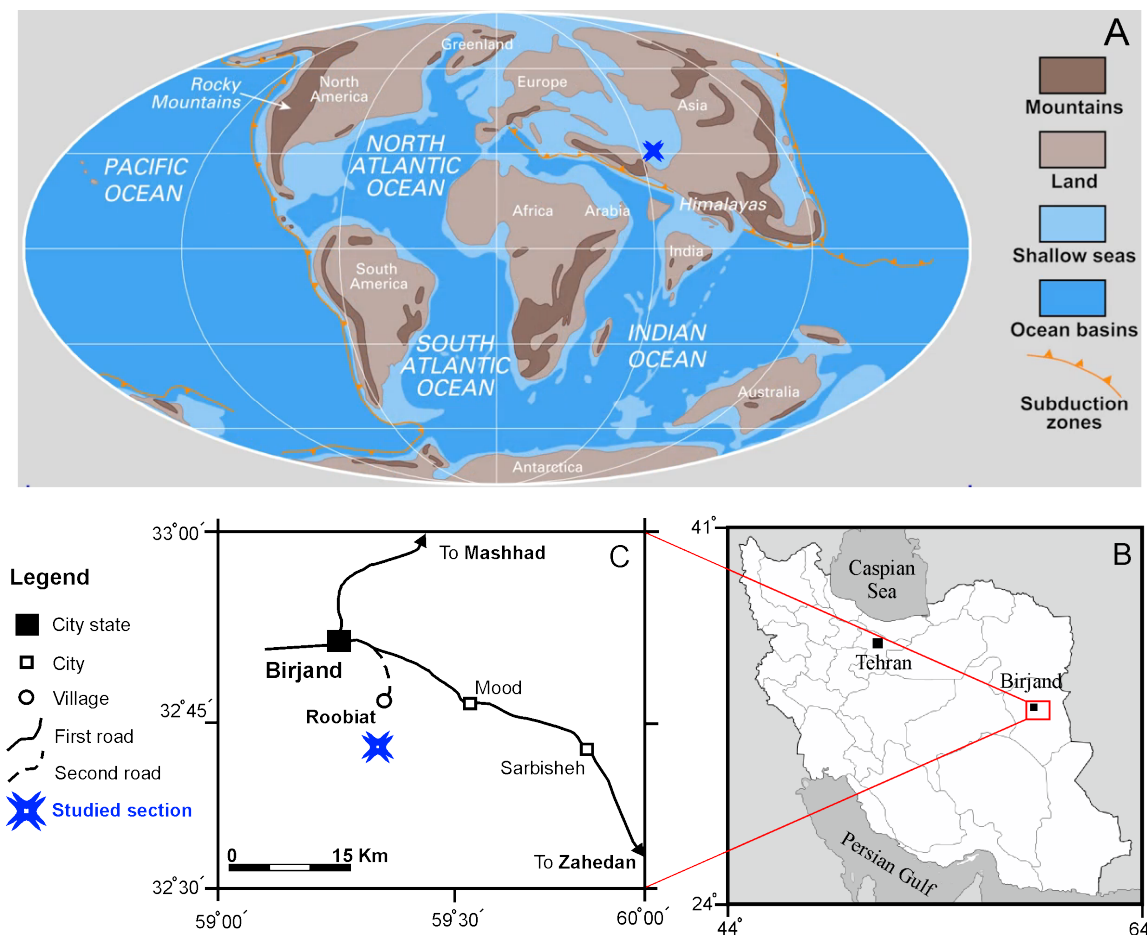


Figure 1. a) Location of the studied section in paleogeographical map through Middle Eocene age (modified after [Scotese, 2013]; b) Position of studied area in Iranian territory; c) The road map of the Roobiat section in Brigand region.

fore, to elucidate the geological position of this part of the Tethys basin, detailed micro-paleontological studies are essential. To investigate the calcareous nannofossils and to perform biostratigraphy, we selected the one of the best outcrop of the sedimentary rock units from the Sistan suture zone, also known as the Roobiat Village section.

2. Material and Methods

The Roobiat stratigraphic section is located in the Northern hemisphere (Figure 1a), Eastern part of Iran (Sistan suture zone) (Figure 1b) to the southeast of Birjand, within the Bagheran Mountains. Its coordinates are 32°42'41" N, 59°16'8" E (Figure 1c). The studied section was 875 m thick and was composed an alternation of the green to gray marlstone and gray shale with intercalation of

thin-bedded sandstone and argillaceous limestone which is deposited on ophiolites-ultramafic rocks and laying under a serpentinized ultramafic rock (Figure 2).

For the calcareous nannofossil studies, 76 rock samples were obtained from marlstone, shale and argillaceous limestone deposits, which were then prepared using the simple smear slide method as described in the literature [Bown and Young, 1998; Parandavar and Hadavi, 2019]. To avoid weathering and its effects, the samples were collected from a depth of 20–30 cm.

The simple smear slide technique is one of the simplest and most inexpensive methods used by different researchers for many years [Lohmann, 1909]. It only needs distilled water to run and no chemicals. After cleaning, the samples, 5 mg of their non-weathered surface is scraped up in to powder on a glass slide and a drop of distilled water is added. Then, the suspended sediment is spread

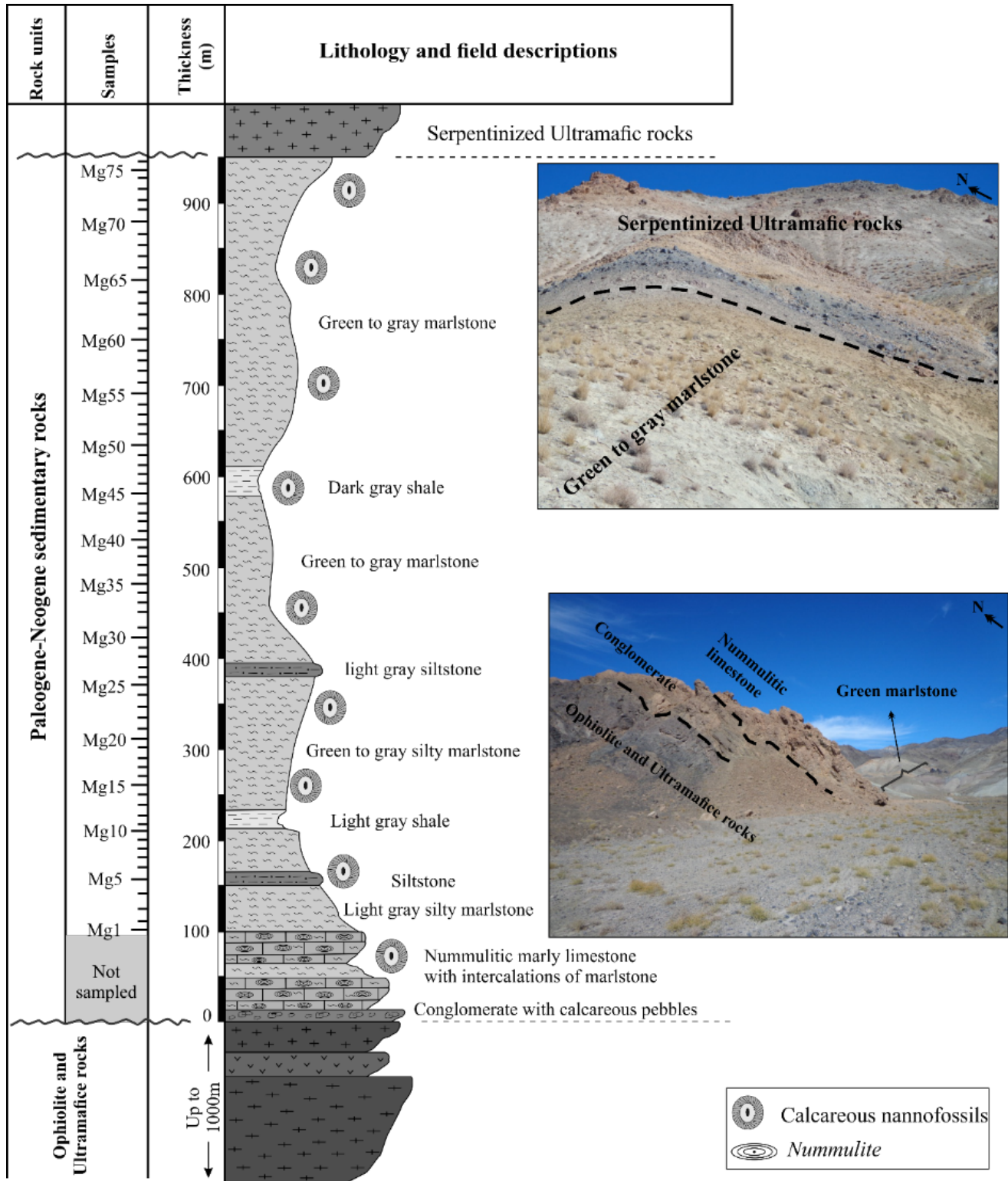


Figure 2. Stratigraphic column of Roobiat section.

across the glass slide with a suitable utensil such as a wooden toothpick and it is finally affixed to the coverslip by Canada balsam adhesive after drying with an electric heater. The prepared slides were studied using an Olympus BX51 polarized light microscope at 1250X magnification and the images of the species were taken by an Olympus DP73 camera. To determine the calcareous nannofossil species, we followed the principles described by *Perch-Nielsen* [1985] and *Bown* [1998].

3. Results

We used according to, the calcareous nannofossils as an efficient tool to determine the age of this section and perform biostratigraphic studies. Due to their small size, coccolithophores are readily preserved as calcareous nannofossils and/or coccoliths, when falling down within the water column [*Bown and Young*, 1998]. The coccoliths are abundant in marine sediments above the calcite compensation depth (CCD): they are usually transported to the seafloor by aggregation of fecal pellets and marine currents [*Bown*, 1998]. They are widely distributed in marine deposits and can be traced within outcropped successions across broad geographic areas. Hence, an examination of the calcareous nannofossil assemblages and separation of time intervals are of grave importance in understanding the structural evolution and regional geology.

In the present study, the investigation of calcareous nannofossil assemblages in the Roobiat section led to the identification of 65 species belonging to 25 genera of this microfossil group (Figure 3). According to the identified index nannofossil species, it has been established that this stratigraphic section had been deposited between NP16 and NN3 biozones of *Martini* [1971] and CP14a to CN2 zones of *Okada and Bukry* [1980]. The distribution pattern of recognized calcareous nannofossil species and detected biozones are shown in Figure 3, and have been compared with the world standard biozonation chart in Figure 4. Also, some of the markers and common nannofossil species are illustrated in Figure 5 and Figure 6. The description of each biozone, is as follows:

***Discoaster tanii-nodifer* Zone (NP16 Zone).** According to the literature, the interval between the Highest Appearance (HA) of *Rhabdoli-*

thus gladius to the HA of *Chiasmolithus solitus* defines this zone [*Perch-Nielsen*, 1985].

Remarks: the NP16 Zone of *Martini* [1971] is one of the interval zones represented the middle Eocene (Lutetian-Bartonian) age [*Agnini et al.*, 2014]. Since *R. gladius* is absent in many areas and is difficult to identify, it is not a useful marker for the basis of the zone [*Fazli and Senemari*, 2018]. However, the same is true for the *C. solitus*, which is especially rare or absent in low latitude sections [*Perch-Nielsen*, 1985]. In this study, too, the *C. solitus* was rare. Nevertheless, sample No. 3 (thickness of 132 m) was assigned to NP16 zone due to the absence of *C. solitus* (Figure 3 and Figure 4).

***Discoaster saipanensis* Zone (NP17 Zone).** Literature defines the NP17 zone of *Martini* [1971] as the interval between the HA of *C. solitus* and the Lowest Appearance (LA) of *Chiasmolithus oamaruensis*.

Remarks: It is difficult to distinguish *D. saipanensis* zone in low latitude areas, where the genus *Chiasmolithus* is rare or absent; therefore, it seems to be thicker than it should [*Perch-Nielsen*, 1985]. So, the successions between samples No. 3 to 8 (thickness of 183 m) with thickness of 51 m. were assigned to the NP17 Zone based on the HAs of *C. solitus* & *C. medius* and the LA of *C. oamaruensis* (Figure 3 and Figure 4).

***Chiasmolithus oamaruensis* Zone (NP18 Zone).** On the base of literature definition, the NP18 Zone of *Martini* [1971] can be considered the interval from the LA of the *C. oamaruensis* to the LA of *Isthmolithus recurvus* species [*Perch-Nielsen*, 1985].

Remarks: In low latitudes, the species belonging to the *Chiasmolithus* and *Isthmolithus* genera, specifically the latter genus, are very rare or often absent. So, it is also difficult to recognize this zone. However, in high latitudes, *Chiasmolithus* and *Isthmolithus* are well dispersed and thus the recognition of this zone poses no problems [*Perch-Nielsen*, 1985]. On the contrary, *Criboecentrum reticulatum* (as synonyms *Reticulofenestra reticulata*) is found throughout NP18 in high and low latitudes which is not worth to as an important event for the definition of this biozone. Due to the absence of *Isthmolithus recurvus*, we could not recognize the upper boundary of the zone. Hence, the NP18 has been intended as a combination with the NP 19 zones in the Roobiat village section (Figure 3).

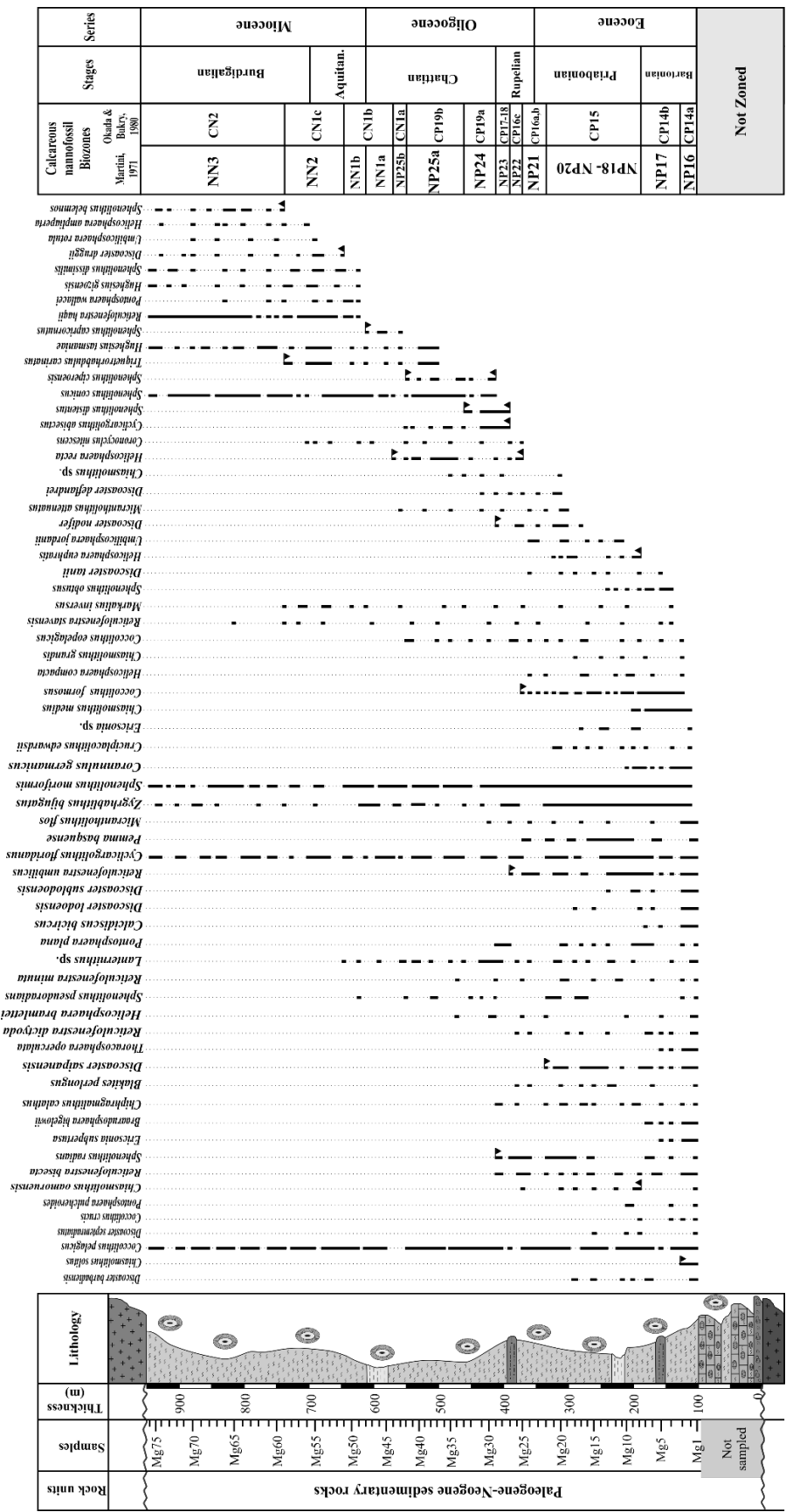


Figure 3. Distribution pattern of calcareous nannofossils and identified the bioevents in the Roobiat section.

Epoch/ Sub Epoch	Stage	Martini 1971 "Cosmopolitan"	Okada and Bukry 1980	Backman et al. 2012	GTS (2020) Events: Agnini et al. (2014) Backman et al. (2012)	This Study								
						Biozones	Nannofossil Events	Biozones						
MIOCENE	Early	Burdigalian	NN3	CN2	CNM5	NN3	<i>S. belemnus</i> <i>T. carinatus</i>	CN2						
									NN2	CN1c	CNM4	NN2	<i>bloom He. carteri</i> common <i>T. carinatus</i> <i>S. disbelemnus</i> <i>D. druggii</i>	CN1c
	Late	Chattian	NN1	CN1a	CNO6	NN1a NP25b	<i>Cy. abisectus</i> <i>S. ciproensis</i>	CN1a						
									NP25	CP19b	CNO5	NP25a	<i>S. distentus</i> <i>S. predistentus</i> <i>S. ciproensis</i>	CP19b
OIGOCENE	Early	Rupelian	NP23	CP18	CNO3	NP23	<i>S. distentus</i> <i>D. nodifer</i> & <i>S. radians</i> <i>Cy. abisectus</i> & <i>S. distentus</i>	CP17-18						
									NP22	CP16c	CNO2	NP22	<i>Re. umbilicus</i> <i>He. recta</i>	CP16c
	Late	Priabonian	NP20	CP15b	CNE21	NP18-20	<i>Cl. subdistichus</i> <i>D. saipanensis</i>	CP15						
									NP19	CP15a	CNE20	NP19	<i>Cr. reticulatum</i> <i>Cr. isabellae</i> <i>Is. recurvus</i>	CP15
Middle	Bartonian	NP17	CP14b	CNE18	NP17	<i>Ch. oamaruensis</i> <i>S. obtusus</i>	CP14b							
								NP16	CP14a	CNE17	NP16	<i>Ch. solitus</i>	CP14a	

Highest Appearance ▼ Lowest Appearance ▲

Figure 4. The detected bioevents and define biozones have been compare with the world standard biozonation charts. Also, some additional and useful bio-events are recorded in here which are traceable from the middle to east of Tethys realm.

***Isthmolithus recurvus* Zone (NP19 Zone).** According to the definition of literature, the interval between the LA of *I. recurvus* and *Sphenolithus pseudoradians* ascertains the NP19 Zone of *Martini* [1971] [Perch-Nielsen, 1985].

Remarks: According to the above mentioned, the *I. recurvus* species is difficult to recognize in low latitudes due to the scarcity [Perch-Nielsen, 1985]. In the present study, owing to the absence of *I. recurvus* we could not separate the lower boundary of the NP19 Zone.

Also, the *S. pseudoradians* can be recognized from older deposited successions which is reported in the newest published studies [e.g. *Bown and Jones, 2012*]. Therefore, this species is not a good biostratigraphic index for define of the upper boundary of this biozone.

Hence, due to the difficulty of the recognition of the lower and upper boundaries, this zone is not

defined, and it is combined with previous (NP18) and later (NP20) zones (Figure 3 and Figure 4).

***Sphenolithus pseudoradians* Zone (NP20 Zone).** In the literature, the NP20 zone of *Martini* [1971] define on the base of LA of the *S. pseudoradians* (in the lower boundary) and HA of the *Discoaster saipanensis* and/or *Discoaster barbadiensis* [Perch-Nielsen, 1985].

Remarks: due to above discussed about *S. pseudoradians*, this species cannot be used as a marker for the distinguishing of the NP19-NP20 boundary. Therefore, this zone has been combined with the NP19 zone (Figure 3 and Figure 4).

Hence, the studied interval from sample No. 8 to 22 (thickness of 336 m) has been considered as a combination of NP18–NP20 zones which is marked with the LAs of *C. oamaruensis* and *Helicosphaera euphratis* at the base and the HA of *D. saipanensis* at the top (Figure 3). This interval have the 153

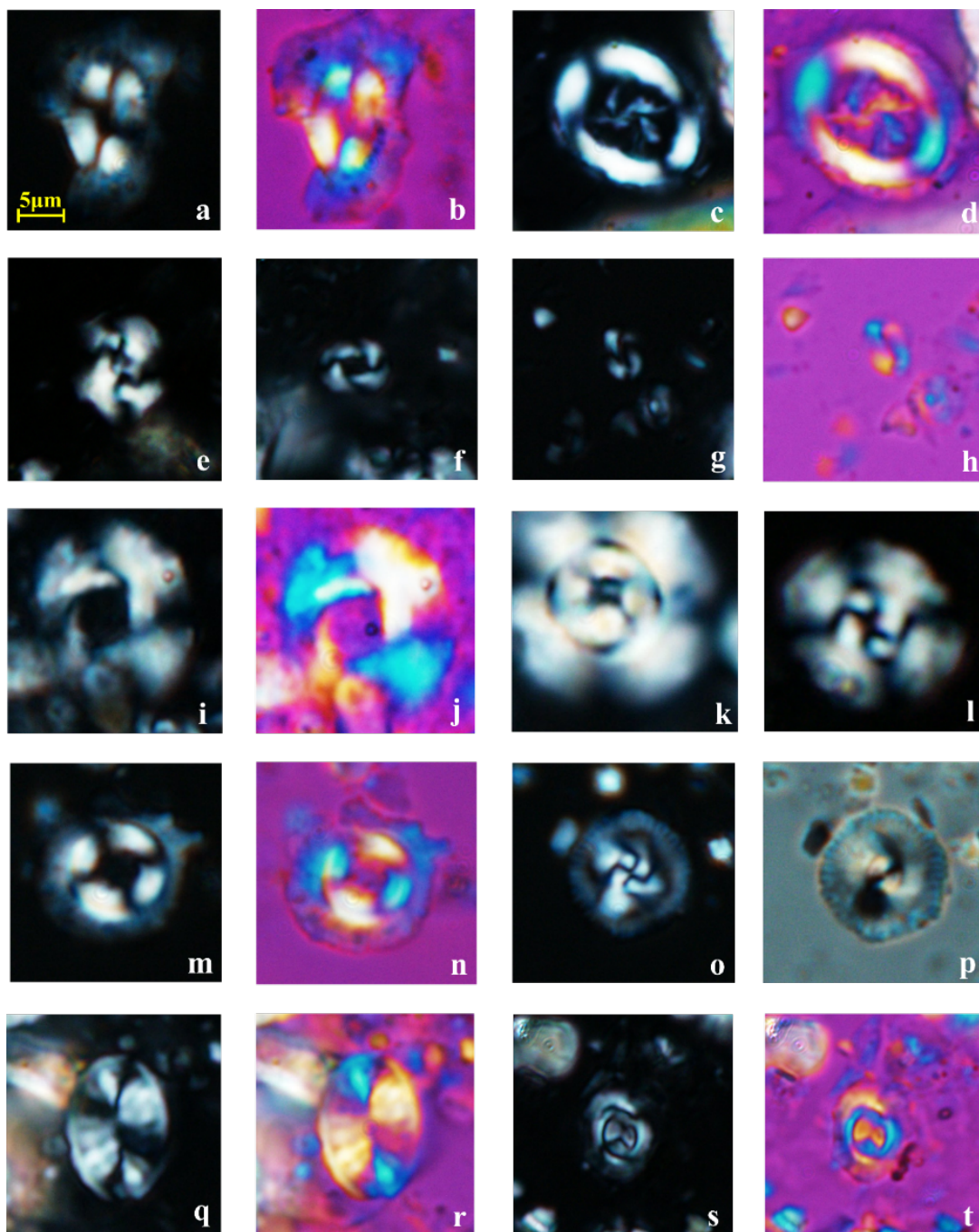


Figure 5. Index and common the calcareous nannofossils observed from the studied sections (scale bar is 5 μm). a–b: *Coccolithus pelagicus* Schiller (fig. a: XPL, fig. b: GW.); c–d: *Chiasmolithus solitus* Locker (figs. c & d: 45°, fig. c: XPL, fig. d: GW); e: *Reticulofenestra bisecta* Roth (fig. e: XPL); f: *Reticulofenestra haqii* Backman (fig. f: XPL); g–h: *Reticulofenestra minuta* Roth (fig. g: XPL, fig. h: GW); i–j: *Reticulofenestra umbilicus* Levin (fig. i: XPL, fig. j: GW); k: *Cyclicargolithus abisectus* Muller (fig. k: XPL); l: *Cyclicargolithus floridanus* Bukry (fig. l: XPL); m–n: *Coccolithus formosus* Wise (fig. m: XPL, fig. n: GW); o–p: *Calcidiscus bicircus* Bown (fig. o: XPL, fig. p: QW); q–r: *Pontosphaera wallacei* Persico (fig. q: XPL, fig. r: GW); s–t: *Hughesius tasmaniae* de Kaenel & Villa (fig. s: XPL, fig. t: GW). QW: Quartz Wedge; GW: Gypsum Wedge.

m thick.

***Ericsonia subdisticha* Zone (NP21 Zone).**

Literature have defined the NP21 Zone of *Martini* [1971] according to the HA of the *Discoaster saipanensis* and/or *Discoaster barbadiensis* at the base, and HA of the *Coccolithus formosus* at the top [Perch-Nielsen, 1985].

Remarks: The disc-shaped *Discoaster* are easily recognizable in the low latitudes and it's a well marker for distinguishing lower boundary, while these nannoliths becomes rare or absent in high latitudes. For determination of the upper boundary of this zone, the HA of the *C. formosus* or *Clausicoccus subdistichus* has been suggested by *Okada and Bukry* [1980] and *Agnini et al.* [2014], respectively (Figure 4). Also, our research shows that these bio-events have been occurred at the same time with the LA of *Helicosphaera recta* (Figure 3). Therefore, this zone has defined by extinction of *D. saipanensis* in the basal boundary, and extinction of *C. formosus* along with the first appearance of the *H. recta* in the upper boundary. Hence, the studied interval between the samples No. 22 and 25 (thickness of 371 m) has been assigned to the NP21 Zone of *Martini* [1971]. This zone with the thickness of 35 m can be comparable with CP16a and CP16b subzones of the *Okada and Bukry* [1980] calcareous nannofossil biozonation pattern which is show the late Eocene (late Priabonian)–early Oligocene (early Rupelian) ages [Agnini et al., 2014] solitus (Figure 3 and Figure 4).

***Helicosphaera reticulata* Zone (NP22 Zone).** According to the definition of literature, the NP22 Zone of *Martini* [1971] was defined from the HA of *C. formosus* to the HA of *Reticulofenestra umbilicus* [Perch-Nielsen, 1985].

Remarks: Although, the *C. formosus* has been continue throughout to the early Oligocene but the extinction of the latter species along with the first appearance of *H. recta* can be a well marker for determination of the lower boundary of the NP22 Zone. The *R. umbilicus* can be occasionally occurred in throughout of the Oligocene succession. Because of this, the upper boundary of the zone will be diachronous.

In the present study, for avoid of create the diachron boundary has been used the LAs of *Sphenolithus distentus* and *Cyclicargolithus abisectus* as along with the HA of *R. umbilicus* (Figure 3). The

NP22 zone of *Martini* [1971] with thickness of 18 m (samples No. 25 to 27) can be comparable with CP16c subzone of the *Okada and Bukry* [1980], which is show the early Oligocene (early Rupelian) age [Agnini et al., 2014] solitus (Figure 3 and Figure 4).

***Sphenolithus predistentus* Zone (NP23 Zone).** Literature define the NP23 Zone of *Martini* [1971] based on the HA of *R. umbilicus* and the LA of *Sphenolithus ciperoensis* [Perch-Nielsen, 1985].

Remarks: In low latitudes, the *Sphenolithus* and *Discoaster* are the best marker for definition of the biozones. Therefore, we have using the HAs of *Sphenolithus radians*, *Discoaster nodifer*, and the LA of the *S. ciperoensis* for define of this zone (Figure 4). Hence, this zone has been assigned to samples No. 27 (thickness of 389 m) to 29 (thickness of 418 m) based on the absence of *R. umbilicus* and the first appearance of *S. ciperoensis*. Also, the zone of NP23 is equivalent to the CP17 and CP18 zones of *Okada and Bukry* [1980] (Figure 4).

***Sphenolithus distentus* Zone (NP24 Zone).** In the literature, the NP24 Zone of *Martini* [1971] define on the base of LA of the *S. ciperoensis* and HA of the *S. distentus* [Perch-Nielsen, 1985].

Remarks: In the present study, the NP24 Zone has been determining on the base of the bio-events belonging to the *S. ciperoensis* and *S. distentus* (Figure 3) which are recorded from sample No. 29 and 33 (thickness of 463 m), respectively. According to *Okada and Bukry* [1980] zonation pattern, the determined biozone can be comparable with the CP19a zone which shows the late Oligocene (Chattian) age [Agnini et al., 2014] (Figure 4).

***Sphenolithus ciperoensis* Zone (NP25 Zone).** According to the definition of literature, the NP25 Zone of *Martini* [1971] can be defined on the base of the HA of *S. distentus* and the HAs of *H. recta* and/or *S. ciperoensis* [Perch-Nielsen, 1985].

Remarks: Previously, although the disappear of the *H. recta* and the *S. ciperoensis* was expressed as a simultaneous event, but the new carried out researches [Agnini et al., 2014]; *Parandavar and Hadavi, 2019* shows that the extinction of these species not to be a synchronous event.

In the present study, the Zone of NP25 has been separated into the two subzones on the base of the time difference between bioevents. The NP25a subzone has defined on the base of the HAs of *S. dis-*

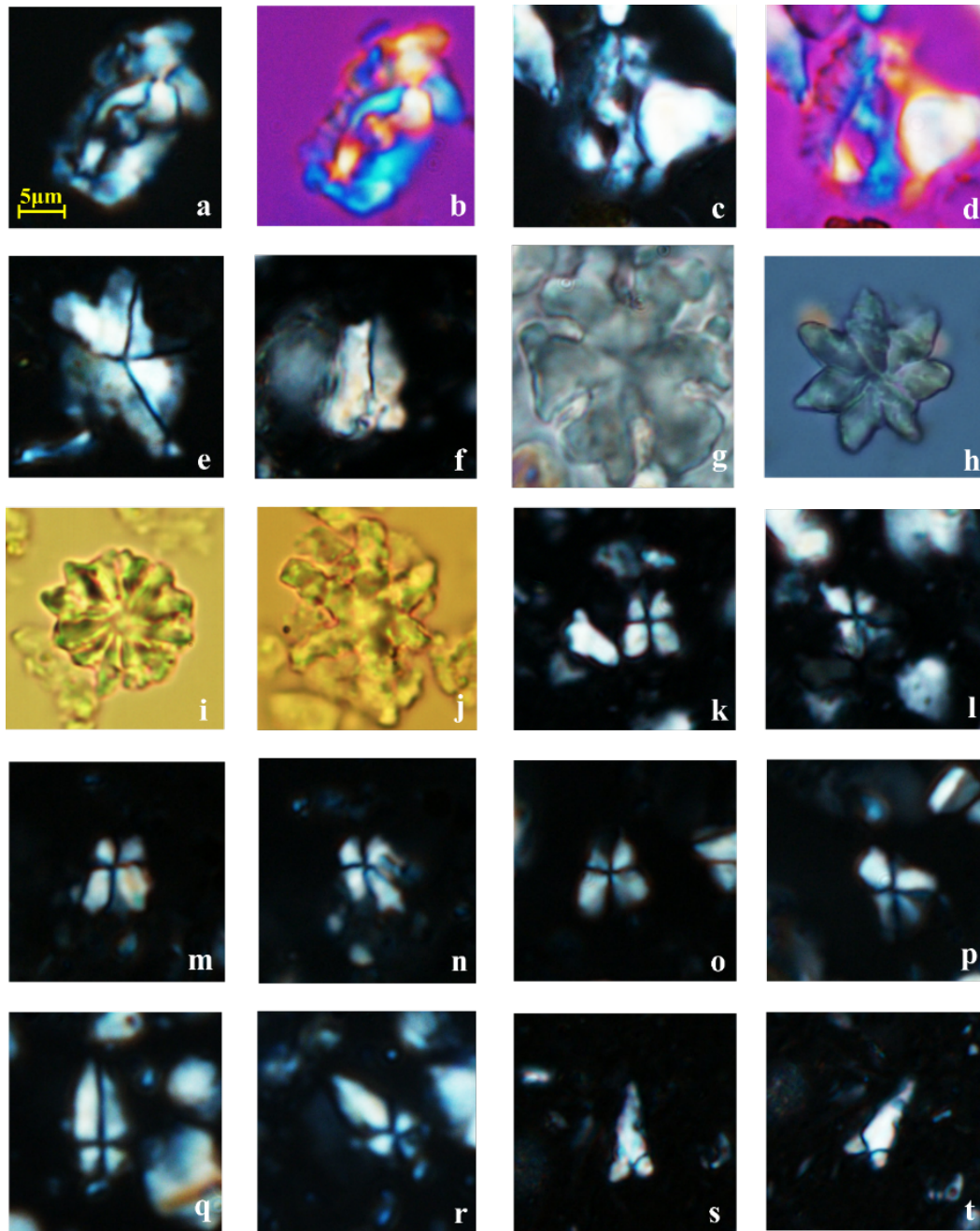


Figure 6. Index and common the calcareous nannofossils observed from the studied sections (scale bar is 5 μm). a–b: *Helicosphaera euphratis* Haq (fig. a: XPL, fig. b: GW); c–d: *Helicosphaera recta* Jafar & Martini (fig. c: XPL, fig. d: GW); e: *Micrantholithus flos* Deflandre (fig. e: XPL); f: *Zygrhablithus bijugatus* Deflandre (fig. f: XPL); g: *Discoaster deflandrei* Bramlette & Riedel (fig. g: QW); h: *Discoaster saipanensis* Bramlette & Riedel (fig. h: QW); i: *Discoaster barbadiensis* Tan 1927 (fig. i: QW); j: *Discoaster nodifer* Bukry (fig. j: QW); k–l: *Sphenolithus belemnos* Bramlette & Wilcoxon (figs. k & l: XPL, fig. k: 0° , fig. l: 45°); m–n: *Sphenolithus disbelemnos* Fornaciari & Rio (figs. m & n: XPL, fig. m: 0° , fig. n: 45°); o–p: *Sphenolithus dissimilis* Bukry & Percival (figs. o & p: XPL, fig. o: 0° , fig. p: 45°); q–r: *Sphenolithus radians* Deflandre (figs. q & r: XPL, fig. q: 0° , fig. r: 45°); s–t: *Sphenolithus ciproensis* Bramlette & Wilcoxon (figs. s & t: XPL, fig. s: 0° , fig. t: 45°). QW: Quartz Wedge; GW: Gypsum Wedge.

tentus (sample No. 33) and *S. ciperoensis* (sample No. 42) species which is equivalent of the CP19b subzone of *Okada and Bukry* [1980]. Also, the interval of between the HAs of *S. ciperoensis* and *H. recta* (sample No. 44) has been assigned to the NP25b subzone. The latter subzone is comparable with the CN1a subzone of *Okada and Bukry* [1980] solitus (Figure 3 and Figure 4). According to the stratigraphic value of the index calcareous nannofossils, the late Oligocene (late Chattian) age can be assigned to the defined subzones.

***Triquetrorhabdulus Carinatus* Zone (NN1 Zone).** Literature has defined the NN1 Zone of *Martini* [1971] on the base of the HA of *H. recta* and/or *S. ciperoensis* and the LA of *Discoaster druggii* [Perch-Nielsen, 1985].

Remarks: According to the newest published researches [e.g. *Agnini et al.*, 2014]; *Parandavar and Hadavi*, 2019], the HA of the *H. recta* occurred at the late Oligocene age and cannot be useful for distinguishing of the Oligocene–Miocene boundary, as already mentioned in the definition of the NN1 Zone by *Martini* [1971]. The HAs of the *Sphenolithus delphix* and/or *Sphenolithus capricornutus* are considered to the closest events to the base of the Miocene [see to *Agnini et al.*, 2014]; *Parandavar and Hadavi*, 2019].

In the present study, the NN1 Zone of *Martini* [1971] has separated into the two subzones of the NN1a and NN1b on the base of the HA of *S. capricornutus* bioevent. The NN1a subzone with thickness of 43 m includes the interval between the HA of the *H. recta* (sample No. 44) and the HA of the *S. capricornutus* (sample No. 48). Also, the determination of the NN1b subzone has been done on the base of the HA of the *S. capricornutus* in the basal boundary (in thickness of 618 m) and the LA of *D. druggii* (sample No. 51; thickness of 645 m) at the top (Figure 3). The ages of late Oligocene (latest Chattian) and early Miocene (earliest Aquitanian) can be assigned to the NN1a and NN1b subzones, respectively. Both of the defined subzones are equivalent to the CN1b subzone of *Okada and Bukry* [1980].

***Discoaster Druggii* Zone (NN2 Zone).** According to the literature, the NN2 zone of *Martini* [1971] has defined on the base of the LA of *D. druggii* and the HA of *Triquetrorhabdulus carinatus* [Perch-Nielsen, 1985].

Remarks: According to the difficult determina-

tion of the *D. druggii* in weak preserved samples, the LA of *Sphenolithus disbelemnus* can be used for definition of the lower boundary [see to *Backman et al.*, 2012]. Also, the *T. carinatus* species may sporadically occur in the low latitude regions. Therefore, it cannot be a credible marker for determination of NN2–NN3 boundary. *Backman et al.* [2012] believe that the LA of the *Sphenolithus belemnus* occurs slightly above the HA of *T. carinatus*, and it can be used to define the top of NN2 Zone.

In the studied section, this zone is defined from sample No. 51 and extends to sample No. 59 (thickness of 738 m) based on the LAs of *D. druggii* and *S. belemnus*. The zone of NN2 with thickness of 93 m is equivalent to the CN1c subzone in the *Okada and Bukry* [1980] zonation which ascertains the Aquitanian–Burdigalian (early Miocene) age [Backman et al., 2012]. As well as, the LA of *Helicosphaera ampliaperta* can be used to determination of the Aquitanian–Burdigalian boundary, according to the *Backman et al.* [2012].

***Sphenolithus belemnus* Zone (NN3 Zone).** The *Martini* [1971] has defined the NN3 Zone based on the interval between the HA of *T. carinatus* to the HA of *S. belemnus*.

Remarks: According to the above mentioned about the *T. carinatus* species, this interval zone can be revised to the total range zone which defines on the base of the LA to HA of *S. belemnus*. Hence, the interval between sample No. 59 to 75 (thickness of 941 m) is related to the NN3 Zone due to the LA of *S. belemnus* along with the HA of *T. carinatus* at the base and the HA of *S. belemnus* at the top. This zone comparable to CN2 Zone of *Okada and Bukry* [1980] which shows the Burdigalian age [Backman et al., 2012].

4. Discussion

Four calcareous nannofossil zonations exist for Paleogene to Neogene deposits. First, *Martini* [1971] established a zonation scheme for the Paleogene (NP zones) and Neogene (NN zones) based mainly upon coastal plain successions. Then, *Bukry* [1973, 1978], *Okada and Bukry* [1980] created the secondary zonation pattern based entirely on deep-sea samples that were collected as part of the Deep

Sea Drilling Project which are named by CP (Paleogene zones) and CN (Neogene zones) codes. Many years later, *Agnini et al.* [2014] and *Backman et al.* [2012] appointed the new zonation schemes as respectively for Paleogene and Neogene series and have been compared them together. According to the published location maps of studied wells and surface sections by above-mentioned authors, most of the sites are located in the western longitudes and regions. So, during the connection between the bio-events in the western regions and the middle to eastern parts of the Tethyan realm, some problems will arise which as following: occur at different time levels; differences in the precedence and latency of bioevents, and etc. Therefore, doing the biostratigraphic studies and define the reference section on a site in the middle part of the Tethys region can improve the differences.

In the present study, we have selected the best outcrop from the eastern part of Iran (Sistan suture zone) that have the most interrelationship with the eastern part of the Tethys realm. According to the biostratigraphic results and what has been described, the biozonal markers are not fully coincident with the literature, and equivalent events must be used, and/or some of the zones can be separated into several subzones. The detected bioevents are traceable from the middle to the east of Tethys region. Although some of this events can be detectable from Mediterranean region.

Here, the biozones have been well described and compared with *Martini* [1971], *Okada and Bukry* [1980], *Backman et al.* [2012] and *Agnini et al.* [2014] zonation schemes (Figure 4). Therefore, the studied section can be appointed as of the reference for the biozonation of the Middle Paleogene to Early Neogene strata. Although it needs to the more investigates which is in doing.

5. Conclusion

In this study, the 25 genera and 65 species of calcareous nannofossils were identified and photographed. The calcareous nannofossil within the studied nannofossil assemblages are present the low variety, well abundance, and medium to good preservation. In the Roobiat Village section, the species have been relatively good preserved, inasmuch as the arms and knobs, the central stem of

the genus *Discoaster*, and also the central area of the genus *Chiasmolithus* were preserved. Moreover, the majority of nannofossils including *Coccolithus*, *Sphenolithus*, *Helicosphaera*, *Reticulofenestra* genera have relatively good preserved. It should be noted that some species have lost their delicate structures due to dissolution. Hence, according to the identified index and common species, the NP16 to NN3 biozones have been determining in throughout the marine successions of the Roobiat section (southeast of Birjand). The identified biozones have suggested the age of middle Eocene (Bartonian) to early Miocene (Burdigalian) for the studied section.

Due to the present study that has been done onto them throughout a succession of the Paleogene to Neogene transition, this section can be recommended as a comparisonal section/region for the correlation between biohorizons from western parts of the Tethys basin and its eastern parts.

Acknowledgments. This study was supported by the Department of Geology from the Ferdowsi University of Mashhad. Accordingly, the authors are grateful to the Ferdowsi University for supplying the samples and analyses required for this study. We would like to acknowledge the Exploration Directorate of NIOC (National Iranian Oil Company) for laboratorial facilities provided.

References

- Aghanabati, A. (2006), *Geology of Iran*, 573 pp. Geological survey of Iran, Tehran.
- Agnini, C., E. Fornaciari, et al. (2014), Biozonation and biochronology of Paleogene calcareous nannofossils from low and middle latitudes, *Newsletters on Stratigraphy*, 47, No. 2, 131–181, **Crossref**
- Backman, J., I. Raffi, et al. (2012), Biozonation and biochronology of Miocene through Pleistocene calcareous nannofossils from low and middle latitudes, *Newsletters on Stratigraphy*, 45, 221–244, **Crossref**
- Berberian, M., G. C. P. King (1981), Towards a paleogeography and tectonic evolution of Iran, *Canadian Journal of Earth Sciences*, 18, 210–265, **Crossref**
- Bown, P. R. (1998), *Calcareous Nannofossils Biostratigraphy*, 315 pp. Kluwer Academic Publishers, Dordrecht. **Crossref**
- Bown, P. R., J. R. Young (1998), Techniques, *Calcareous Nannofossil Biostratigraphy*, P. R. Bown

- (Ed.) p. 16–28, Kluwer Academic Publishers, Dordrecht. **Crossref**
- Bown, P. R., D. T. Jones (2012), Calcareous nanofossils from the Paleogene equatorial Pacific (IODP Expedition 320 Sites U1331-1334), *Journal of Nanoplankton Research*, 32, No. 2, 3–51.
- Bukry, D. (1973), Low-latitude coccolith biostratigraphic zonation, *Initial Reports of the Deep Sea Drilling Project*, 15, 685–703, **Crossref**
- Bukry, D. (1978), Biostratigraphy of Cenozoic marine sediments by calcareous nanofossils, *Micropaleontology*, 24, 44–60, **Crossref**
- Fazli, L., S. Senemari (2018), Calcareous nanofossil biostratigraphy of the Eocene of the Zagros Basin in Iran, *Neues Jahrbuch für Geologie und Paläontologie, Abhandlungen*, 287, No. 2, 143–151, **Crossref**
- Hadavi, F., M. Notghi Moghaddam, L. Khodadadi (2016), Biostratigraphy and paleoecology of Cretaceous rocks based on calcareous nanofossil in Sarayan section, East Iran, *Iranian Journal of Earth Sciences*, 8, No. 1, 52–68.
- Jalili, F., M. Notghi Moghaddam, F. Hadavi (2020), Investigation of the Silak Section Filyschoid deposits based on calcareous nanofossils and comparison with Shushud and Sarayan sections (East Lut Block), *Kharazmi Journal of Earth Sciences*, 5, No. 2, 159–174, **Crossref**
- Lohmann, H. (1909), Die Gehäuse und Gallenblasen der Appendikularien und ihre Bedeutung für die Erforschung des Lebens im Meer, *Verh. Dtsch. Zool. Ges.*, 19, 200–233.
- Martini, M. (1971), Standard Tertiary and Quaternary Calcareous Nannoplankton Zonation, *Proc. of the 2nd Planktonic Conference Roma*, 2, 739–785.
- Okada, H., D. Bukry (1980), Supplementary modification and introduction of code numbers to the low-latitude coccolith biostratigraphic zonation, *Marine Micropaleontology*, 5, 321–325, **Crossref**
- Parandavar, M., F. Hadavi (2019), Identification of the Oligocene-Miocene boundary in the Central Iran Basin (Qom Formation): Calcareous nanofossil evidences, *Geological Quarterly*, 62, No. 2, 215–229, **Crossref**
- Perch-Nielsen, K. (1985), Cenozoic Calcareous Nanofossils, *Plankton Stratigraphy*, H. M. Bolli, J. B. Sanders & K. Perch-Nielsen (Eds.) p. 427–554, Cambridge University Press, Cambridge.
- Scotese, C. R. (2013), *Paleogeography*, Encyclopaedia Britannica publisher, Edinburgh. (<https://www.britannica.com/science/paleogeography>)
- Tirrul, R., I. K. Bell, et al. (1983), The Sistan suture zone of eastern Iran, *Geological Society of American, Bulletin*, 94, 134–150, (in Russian) **Crossref**

Corresponding author:

Mina Ghavidel Darestani, Department of Geology, Faculty of Sciences, Ferdowsi University of Mashhad, Mashhad, Iran. (mina.ghavidel@gmail.com & parandavar.m@gmail.com)